**The EMBO Journal** Vol. 20 No. 4 pp. 777–791, 2001

# The budding yeast proteins Spc24p and Spc25p interact with Ndc80p and Nuf2p at the kinetochore and are important for kinetochore clustering and checkpoint control

**Carsten Janke, Jennifer Ortiz[1], Johannes Lechner[1], Anna Shevchenko[2], Andrej Shevchenko[2], Maria M.Magiera, Carolin Schramm and Elmar Schiebel[3]**

The Beatson Institute for Cancer Research, CRC Beatson Laboratories, Glasgow G61 1BD, UK, [1]Biochemistry Center, Ruprecht-Karls University, 69120 Heidelberg and [2]Peptide and Protein Group, European Molecular Biology Laboratory, 69012 Heidelberg, Germany

[3]Corresponding author
e-mail: eschiebe@udcf.gla.ac.uk

**Here, we show that the budding yeast proteins Ndc80p, Nuf2p, Spc24p and Spc25p interact at the kinetochore. Consistently, Ndc80p, Nuf2p, Spc24p and Spc25p associate with centromere DNA in chromatin immunoprecipitation experiments, and *SPC24* interacts genetically with *MCM21* encoding a kinetochore component. Moreover, although conditional lethal *spc24-2* and *spc25-7* cells form a mitotic spindle, the kinetochores remain in the mother cell body and fail to segregate the chromosomes. Despite this defect in chromosome segregation, *spc24-2* and *spc25-7* cells do not arrest in metaphase in response to checkpoint control. Furthermore, *spc24-2* cells showed a mitotic checkpoint defect when microtubules were depolymerized with nocodazole, indicating that Spc24p has a function in checkpoint control. Since Ndc80p, Nuf2p and Spc24p are conserved proteins, it is likely that similar complexes are part of the kinetochore in other organisms.**

*Keywords*: kinetochore/Ndc80p/Nuf2p/Spc24p/Spc25p

## Introduction

The centromere–kinetochore complex ensures high-fidelity chromosome segregation in mitosis and meiosis by mediating the attachment and movement of chromosomes along spindle microtubules (Pidoux and Allshire, 2000). Kinetochores from different organisms vary widely in terms of length. In fission yeast, the centromere DNA is 40–100 kbp (Takahashi *et al*., 1992) and in mammalian cells up to 1000 kbp long. In contrast, the centromere DNA of budding yeast is a relatively simple assembly of 125 bp (Fitzgerald-Hayes *et al*., 1982).

A number of budding yeast kinetochore proteins are conserved. Cse4p, a histone H3 variant, is a component of the core centromere of *Saccharomyces cerevisiae* and shows homology to the human centromere protein CENP-A (Meluh *et al*., 1998). Mif2p is another conserved component of the yeast kinetochore that displays similarity to mammalian CENP-C (Meluh and Koshland, 1995). Additional budding yeast core kinetochore components are Ndc10p, Cep3p, Ctf13p and Skp1p, which form the CBF3 subcomplex (Lechner and Carbon, 1991; Goh and Kilmartin, 1993; Lechner, 1994; Stemmann and Lechner, 1996). A further subcomplex, composed of Ctf19p, Mcm21p and Okp1p, localizes to yeast centromere DNA in a CBF3-dependent manner (Ortiz *et al*., 1999). Similarly, centromere association of Mtw1p, a homologue of the fission yeast kinetochore protein Mis12, was dependent on Ndc10p (Goshima and Yanagida, 2000).

In *S.cerevisiae*, sister centromeres undergo cycles of splitting and rejoining at the end of S-phase, while the chromosome arms remain attached until the metaphase to anaphase transition (Goshima and Yanagida, 2000; He *et al*., 2000; Tanaka *et al*., 2000). This separation is probably due to forces exerted at the sister kinetochores after bipolar attachment to the mitotic spindle (Goshima and Yanagida, 2000). As a result of these forces, the cohesin complexes that establish sister chromatid cohesion probably disassemble or are displaced from the kinetochore, while the complexes localized along the chromosome arms remain bound (Tanaka *et al*., 2000).

The budding yeast kinetochores are clustered throughout the cell cycle near the microtubule organizing centre, known as the spindle pole body (SPB) (Goh and Kilmartin, 1993; Hyland *et al*., 1999; Goshima and Yanagida, 2000; He *et al*., 2000; Jin *et al*., 2000; Tanaka *et al*., 2000). Measurements of the distance between the yeast γ-tubulin, named Tub4p, which is associated with the nuclear side of the SPB (Spang *et al*., 1996), and Mtw1p, a centromere component, revealed that kinetochores of fixed cells are on average only ~0.3–0.4 μm apart from the SPB (Goshima and Yanagida, 2000). Time-lapse experiments using the central SPB component Spc42p (Donaldson and Kilmartin, 1996) as an SPB marker indicated that the distance between the SPB core and the kinetochore fluctuates between 0.5 and 2.5 μm before onset of anaphase B. During anaphase B, the distance between the SPB and the kinetochore is relatively constant, at 0.5–1 μm (He *et al*., 2000; Tanaka *et al*., 2000).

Proteins close to the inner plaque of the SPB, which organizes the nuclear microtubules, have been identified upon isolation of SPBs (Wigge *et al*., 1998). We have analysed some of these proteins and found that Ndc80p (Rout and Kilmartin, 1990), Nuf2p (Osborne *et al*., 1994), Spc24p and Spc25p (Wigge *et al*., 1998) interact at the kinetochore. Moreover, our data suggest that at least Spc24p and Spc25p have a role in spindle checkpoint control and in centromere clustering. Interestingly, homologues of Ndc80p, Nuf2p and Spc24p are present in other organisms, raising the

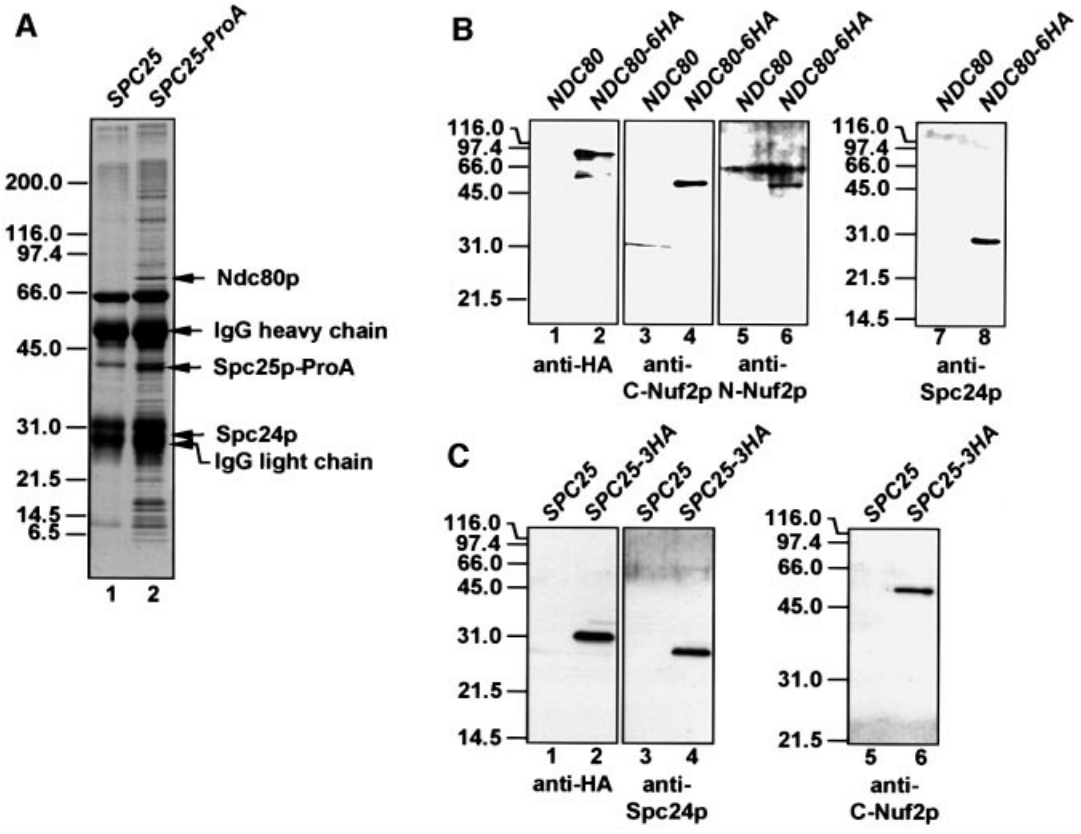


**Fig. 1.** Ndc80p, Nuf2p, Spc24p and Spc25p are present in common complexes. (**A**) Purification of Spc25p-associated proteins. Magnetic beads coated with rabbit IgGs were incubated with a yeast extract of wild-type (lane 1) or *SPC25–ProA* cells (lane 2). Bound proteins were eluted and separated by SDS–PAGE. Coomassie Blue-stained proteins were analysed by MALDI analysis. The major protein bands were identified as Ndc80p, Spc25p–ProA and Spc24p. The minor bands were contaminants like ribosomal proteins. (**B**) Co-immunoprecipitation of Ndc80p, Nuf2p and Spc24p. Extracts of *NDC80* (lanes 1, 3, 5 and 7) or *NDC80-6HA* cells (lanes 2, 4, 6 and 8) were incubated with anti-HA beads. The precipitate was analysed by immunoblotting using anti-HA (lanes 1 and 2), anti-C-Nuf2p (lanes 3 and 4), anti-N-Nuf2p (lanes 5 and 6) and anti-Spc24p antibodies (lanes 7 and 8). (**C**) Co-immunoprecipitation of Nuf2p and Spc24p with Spc25p-6HA. The experimental design was as in (B), using *SPC25* (lanes 1, 3 and 5) and *SPC25-3HA* cell extract (lanes 2, 4 and 6). The precipitates were tested with anti-HA (lanes 1 and 2), anti-Spc24p (lanes 3 and 4) and anti-C-Nuf2p antibodies (lanes 5 and 6).

possibility that these proteins are also associated with the kinetochore.

## Results

### *Purification of Spc25p reveals complex formation with Ndc80p, Nuf2p and Spc24p*

Spc25p is a protein of unknown function that co-purifies with budding yeast SPBs (Wigge *et al*., 1998). In order to understand the role of Spc25p, a functional, chromosomal gene fusion of *SPC25* and protein A (ProA) was constructed. The Spc25p–ProA fusion protein was purified from yeast cell extracts using magnetic beads coated with IgGs, to which ProA binds with high affinity. As a control for proteins that bind non-specifically, an extract from cells without a ProA tag was incubated with the IgG beads. Proteins that were present in the Spc25p–ProA purification (Figure 1A, lane 2) but not in the control (lane 1) were analysed by matrix-assisted laser desorption/ionization (MALDI) analysis (Shevchenko *et al*., 1996). The strong protein bands of ~30, 42 and 80 kDa were identified as Spc24p, Spc25p–ProA and Ndc80p. Ndc80p, Spc24p and Spc25p are proteins of unknown function, which are associated with the nuclear side of the SPB (Rout and Kilmartin, 1990; Wigge *et al*., 1998).

To confirm complex formation of these proteins, Ndc80p-6HA and Spc25p-3HA were immunoprecipitated using anti-haemagglutinin (HA) antibodies. As shown by immunoblotting, Spc24p (Figure 1B, lane 8, and C, lane 4) co-immunoprecipitated with Ndc80p-6HA (Figure 1B, lane 2) and Spc25p-3HA (Figure 1C, lane 2). We also excluded the possibility that entire SPBs or larger SPB subcomplexes were precipitated by the anti-HA antibodies. Spc72p, a component of the outer plaque (Knop and Schiebel, 1998), Spc110p, which binds to the γ-tubulin complex at the inner plaque (Knop and Schiebel, 1997), γ-tubulin (Tub4p) (Spang *et al*., 1996) and β-tubulin (Tub2p) (Neff *et al*., 1983) were not detected in the immunoprecipitate (not shown). Surprisingly, Nuf2p, an SPB-associated protein (Osborne *et al*., 1994) was identified in the Ndc80p-6HA precipitate by antibodies directed against the N-terminal (Figure 1B, lane 6) and C-terminal domain of Nuf2p (Figure 1B, lane 4). This suggested that Nuf2p interacts with Ndc80p, Spc24p or Spc25p. Nuf2p was probably not found in the Spc25p–ProA purification (Figure 1A, lane 2) because

**Table I.** Genetic interactions of *NDC80*, *NUF2*, *SPC24* and *SPC25*

| Mutant | pRS426 with | Growth at the indicated temperature | | | | |
|---|---|---|---|---|---|---|
| | | 23°C | 30°C | 33°C | 35°C | 37°C |
| *nuf2-61* | *NDC80* | +++ | +++ | – | – | – |
| | *NUF2* | +++ | +++ | +++ | +++ | +++ |
| | *SPC24* | +++ | +++ | + | – | – |
| | *SPC25* | +++ | +++ | + | – | – |
| | *SPC98* | +++ | +++ | – | – | – |
| | no insert | +++ | +++ | – | – | – |
| *ndc80-1* | *NDC80* | +++ | +++ | +++ | +++ | +++ |
| | *NUF2* | +++ | +++ | – | – | – |
| | *SPC24* | +++ | +++ | + | – | – |
| | *SPC25* | +++ | +++ | + | – | – |
| | *SPC98* | +++ | +++ | – | – | – |
| | no insert | +++ | +++ | – | – | – |
| *ndc80-2* | *NDC80* | +++ | +++ | +++ | +++ | +++ |
| | *NUF2* | +++ | +++ | +++ | – | – |
| | *SPC24* | +++ | +++ | +++ | + | – |
| | *SPC25* | +++ | +++ | +++ | – | – |
| | *SPC98* | +++ | +++ | +++ | – | – |
| | no insert | +++ | +++ | +++ | – | – |
| *spc24-2* | *NDC80* | +++ | +++ | + | – | – |
| | *NUF2* | +++ | +++ | + | – | – |
| | *SPC24* | +++ | +++ | +++ | +++ | +++ |
| | *SPC25* | +++ | +++ | +++ | – | – |
| | *SPC98* | +++ | +++ | + | – | – |
| | no insert | +++ | +++ | + | – | – |
| *spc24-3* | *NDC80* | +++ | +++ | +++ | + | – |
| | *NUF2* | +++ | +++ | +++ | + | – |
| | *SPC24* | +++ | +++ | +++ | +++ | +++ |
| | *SPC25* | +++ | +++ | +++ | +++ | +++ |
| | *SPC98* | +++ | +++ | +++ | + | – |
| | no insert | +++ | +++ | +++ | + | – |
| *spc25-4* | *NDC80* | +++ | +++ | +++ | + | – |
| | *NUF2* | +++ | +++ | +++ | – | – |
| | *SPC24* | +++ | +++ | +++ | +++ | +++ |
| | *SPC25* | +++ | +++ | +++ | +++ | +++ |
| | *SPC98* | +++ | +++ | +++ | – | – |
| | no insert | +++ | +++ | +++ | – | – |
| *spc25-7* | *NDC80* | +++ | +++ | + | – | – |
| | *NUF2* | +++ | +++ | – | – | – |
| | *SPC24* | +++ | +++ | + | – | – |
| | *SPC25* | +++ | +++ | +++ | +++ | +++ |
| | *SPC98* | +++ | +++ | – | – | – |
| | no insert | +++ | +++ | – | – | – |

High gene dosage suppression was tested as described in Materials and methods.
–, no growth; +, reduced growth; +++, normal growth.

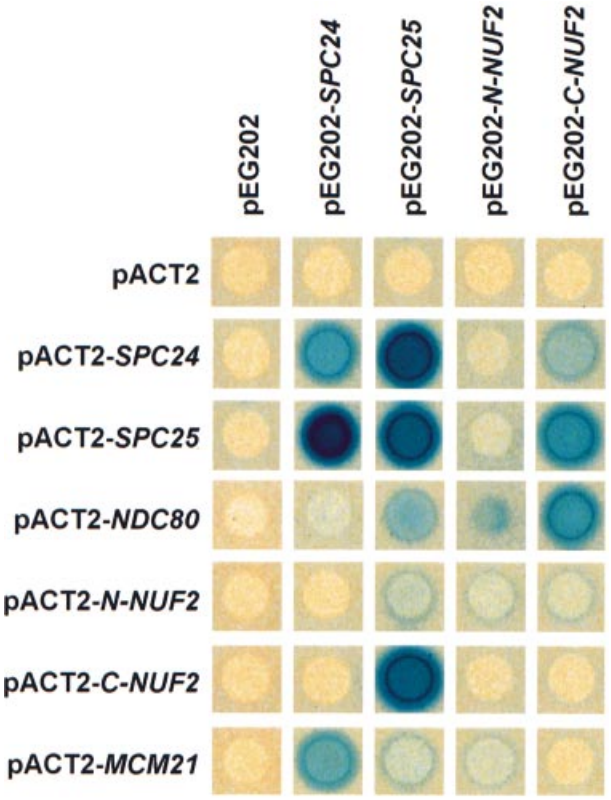


**Fig. 2.** Ndc80p, Nuf2p, Mcm21p, Spc24p and Spc25p interact in the yeast two-hybrid system. Yeast strains containing the indicated yeast two-hybrid plasmids were overlayed with top agar containing 5-bromo-4-chloro-3-indolyl-β-D-galactoside (X-Gal) to measure β-galactosidase activity. Plates were incubated for 6 h at 30°C. Blue colour indicates interaction.

the eluted IgG heavy chain overlapped with the 53 kDa Nuf2p band. To confirm this notion, the Spc25p-3HA precipitate was tested for Nuf2p. Indeed, Nuf2p (Figure 1C, lane 6) co-immunoprecipitated with Spc25p-3HA (lane 2). All these precipitations were specific, since no co-immunoprecipitations were observed when control strains without a tag were used (Figure 1B, lanes 1, 3, 5 and 7, and C, lanes 1, 3 and 5). In conclusion, Ndc80p, Nuf2p, Spc25p and Spc24p are present in common complexes.

### *NDC80, NUF2, SPC24 and SPC25 function together*

To confirm that *NDC80*, *NUF2*, *SPC25* and *SPC24* function together *in vivo*, we investigated whether the four genes interact genetically. Multiple genetic interactions were observed when conditional lethal *NDC80*, *NUF2*, *SPC24* or *SPC25* cells were tested for high gene dosage suppression (Table I). The growth defect of *spc24-3* and *spc25-4* cells at 37°C was strongly suppressed by high gene dosage of *SPC25* or *SPC24*, respectively. In contrast, multiple copies of *SPC25* suppressed the growth defect of *spc24-2* cells only at 33°C, but not at higher temperatures (Table I), indicating that the extent of suppression is allele specific. Somewhat weaker suppressions were observed of *nuf2-61* cells by *SPC24* and *SPC25*, of *ndc80-1* cells by *SPC24* and *SPC25*, of *spc25-4* cells by *NDC80*, and of *spc25-7* cells by *NDC80* and *SPC24*. As a control for the specificity of the suppression, we tested *SPC98*, coding for a subunit of the yeast γ-tubulin complex that is located at the inner plaque of the SPB, as are Ndc80p, Spc24p and Spc25p (Geissler *et al*., 1996). *SPC98* had no influence on the growth of the temperature-sensitive *ndc80(ts)*, *nuf2(ts)*, *spc24(ts)* or *spc25(ts)* cells (Table I).

Strong two-hybrid interactions were detected between Ndc80p and the C-terminal domain of Nuf2p (C-Nuf2p), Spc24p and Spc25p, and C-Nuf2p and Spc25p. C-Nuf2p and Spc24p, Ndc80p and Spc25p, and Ndc80p and N-Nuf2p showed weaker interactions (Figure 2). Some of these two-hybrid interactions have been identified previously (Cho *et al*., 1998). When taken together, our genetic data suggest that Ndc80p, Nuf2p, Spc24p and Spc25p function together *in vivo*.

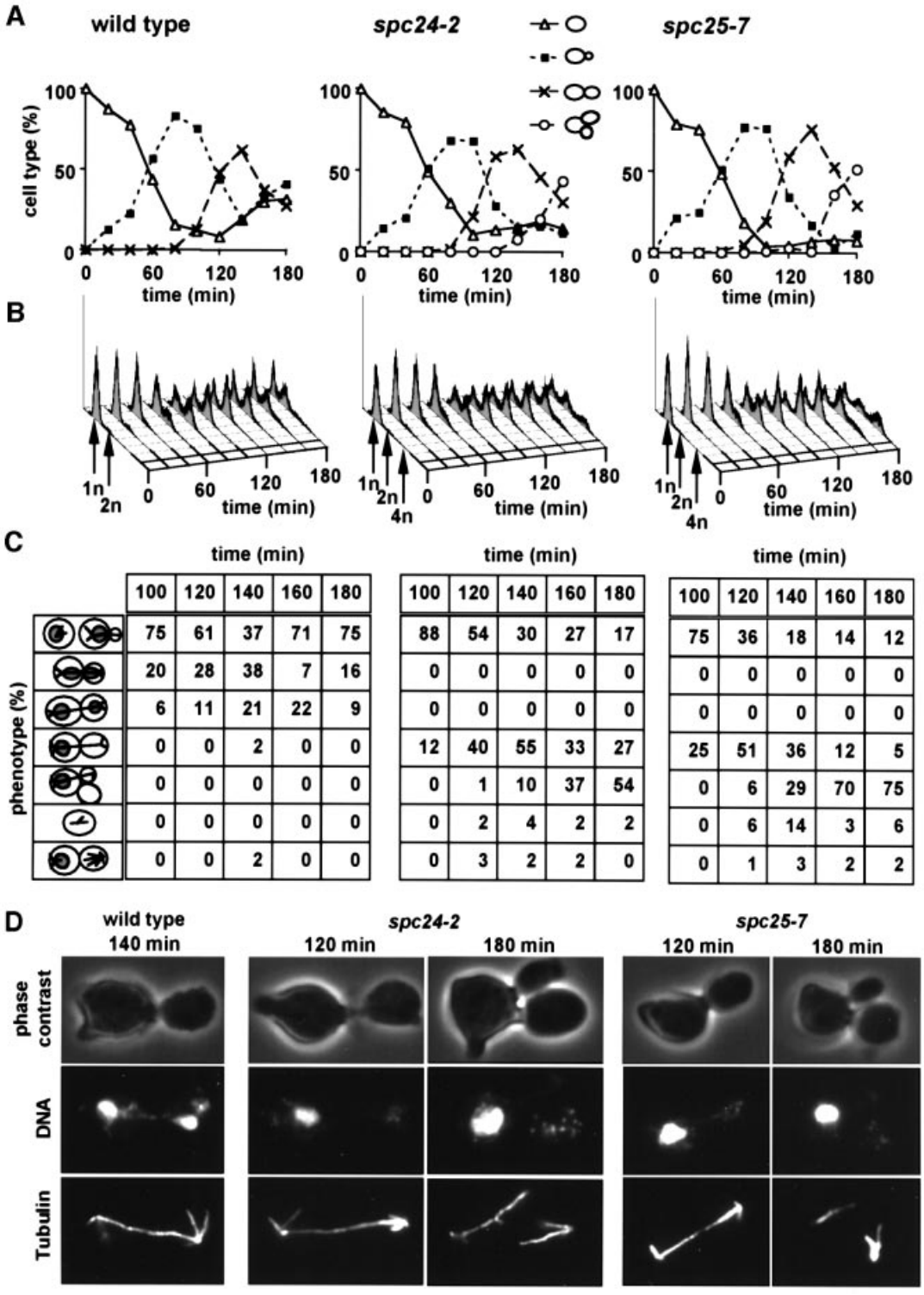


**Fig. 3.** *spc24-2* and *spc25-7* cells form an anaphase spindle but fail to segregate the chromosomes. Wild-type, *spc24-2* and *spc25-7* cells were synchronized with α-factor. The block was released and the cells were shifted to the restrictive temperature. Samples were withdrawn every 20 min and analysed for (**A**) budding index and (**B**) DNA content by flow cytometry. (**C** and **D**) Indirect immunofluorescence with anti-tubulin antibodies and 4′-6-diamidine-2-phenylindole (DAPI) staining. (C) is the quantification of (D) ($n$ = 200). (C) In the cartoons at the left side of the panel, the grey circles within the cells symbolize the DAPI staining regions, and the lines the microtubules. Note that only the cell types after 100 min incubation at 37°C are shown.

### *spc24-2 and spc25-7 cells are defective in chromosome segregation and checkpoint control*

The function of *SPC24* and *SPC25* was investigated by analysing the phenotype of conditional lethal mutants. Synchronized wild-type, *spc24-2* and *spc25-7* cells ($t$ = 0) were shifted to 37°C. *spc24-2* and *spc25-7* cells replicated their DNA and formed a bud with similar kinetics to wild-type cells (Figure 3A–C).

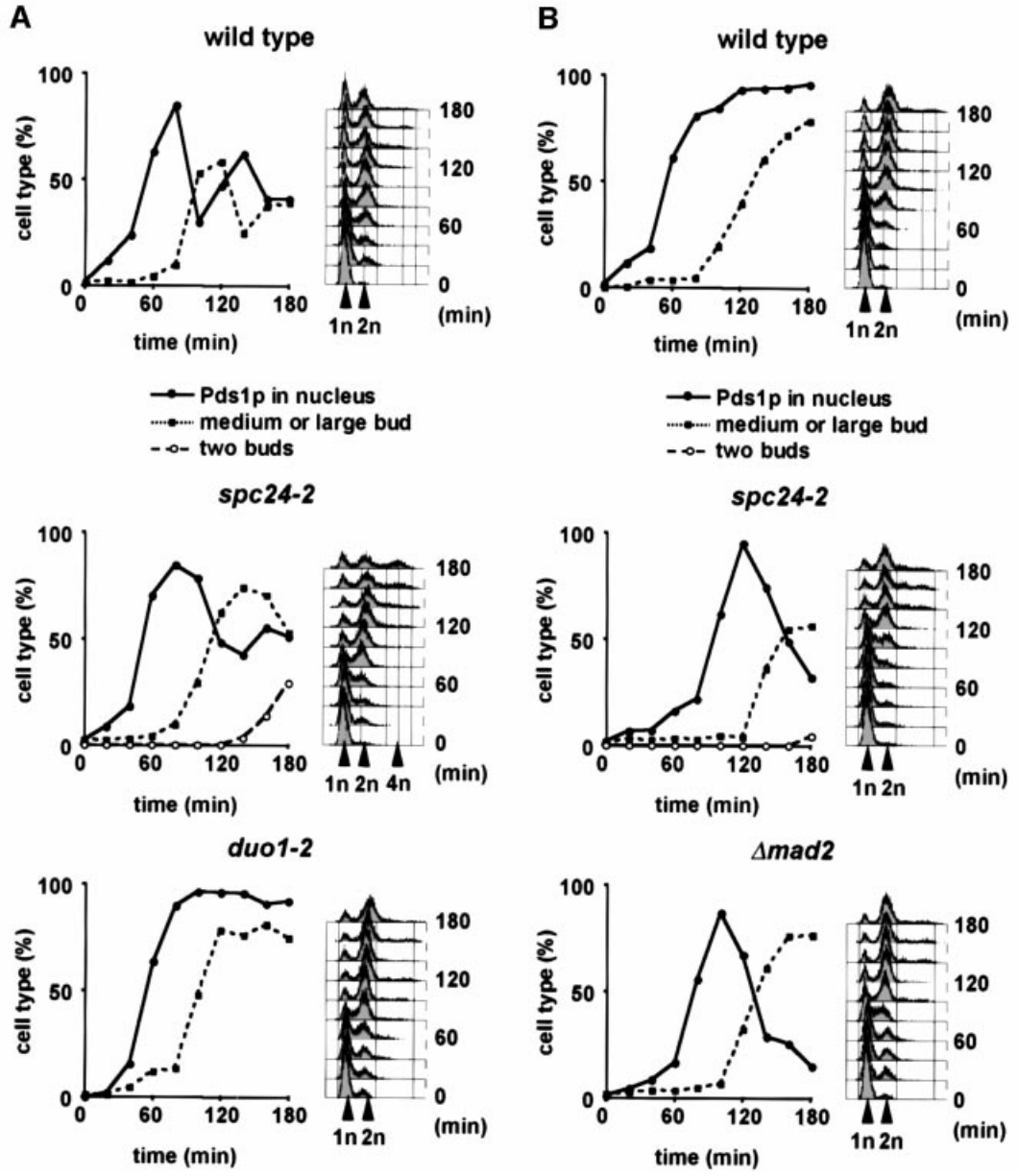


**Fig. 4.** *spc24-2* cells are checkpoint deficient. (A and B) α-factor synchronized wild-type, *spc24-2*, *duo1-2* or *Δmad2* cells containing *PDS1-6HA* were shifted to 37°C with (**B**) or without (**A**) 15 μg/ml nocodazole. Samples were withdrawn every 20 min and analysed for budding index, nuclear Pds1p by immunofluorescence, and DNA content by flow cytometry. Cells were also stained with anti-tubulin antibodies to ensure microtubule depolymerization when incubated with nocodazole.

However, in contrast to wild-type cells, chromosome segregation of *spc24-2* and *spc25-7* cells was disturbed (Figure 3C and D). In wild-type cells, separation of DNA masses coincided with the formation of an anaphase spindle (Figure 3D, wild type). In *spc24-2* (Figure 3D, *spc24-2*, 120 min) and *spc25-7* cells (Figure 3D, *spc25-7*, 120 min), the chromosomal DNA remained in the mother cell (cell with mating projection), despite the formation of an anaphase spindle. Moreover, many *spc24-2* and *spc25-7* cells did not arrest in the cell cycle, as indicated by the re-replication of the DNA (Figure 3B, 4n peak after 160–180 min) and the formation of an additional bud (Figure 3C and D, *spc24-2* and *spc25-7*, 180 min). Thus, *spc24-2* and *spc25-7* cells are defective in chromosome segregation and fail to arrest in the cell cycle.

The degradation of Pds1p via the anaphase promoting complex and the proteasome at the metaphase to anaphase transition is inhibited upon activation of the Mad2p-dependent checkpoint (hereafter named the Mad2p checkpoint) (Hwang *et al*., 1998). To determine whether *spc24-2* cells are Mad2p checkpoint deficient, we investigated the kinetics of Pds1p degradation of synchronized *PDS1-6HA* and *spc24-2 PDS1-6HA* cells incubated at 37°C. *duo1-2 PDS1-6HA* cells, which arrest in metaphase due to Mad2p checkpoint activation (Hofmann *et al*., 1998), were used as a control. Whereas *duo1-2* cells arrested in the cell cycle

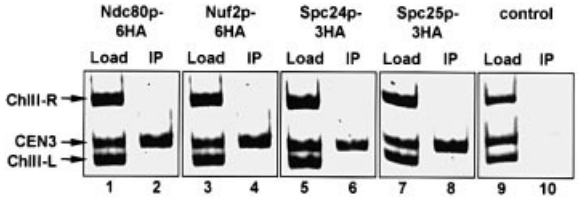


**Fig. 5.** Ndc80p, Nuf2p, Spc24p and Spc25p are associated with the budding yeast kinetochore. *NDC80-6HA* (lanes 1 and 2), *NUF2-6HA* (lanes 3 and 4), *SPC24-3HA* (lanes 5 and 6) and *SPC25-3HA* cells (lanes 7 and 8), and wild-type cells without an HA tag (lanes 9 and 10) were subjected to ChIP. The immunoprecipitation was tested for the presence of CEN3 DNA and fragments left (ChIII-L) and right (ChIII-R) of CEN3 (IP: lanes 2, 4, 6, 8 and 10), as described previously (Ortiz *et al*., 1999). As a positive control for the PCR reactions, yeast lysates were tested without anti-HA precipitation (Load: lanes 1, 3, 5, 7 and 9).

with stable Pds1p after ~80 min, wild-type cells degraded the nuclear Pds1p before the occurrence of large buds (Figure 4A, wild type, decline of Pds1p after 80 min). *spc24-2* cells also degraded the nuclear Pds1p, but were slightly delayed by ~20 min compared with wild-type cells (Figure 4A, *spc24-2*, Pds1p strongly declined after 100 min). Furthermore, re-replication and bud formation of *spc24-2* cells further indicated cell cycle progression (see flow cytometry and cells with two buds in Figure 4A, *spc24-2*). Together, these results suggest that the mitotic checkpoint is impaired in *spc24-2* cells.

The checkpoint defect of *spc24-2* cells was investigated further by following cell cycle progression of synchronized *PDS1-6HA*, *spc24-2 PDS1-6HA* and *Δmad2 PDS1-6HA* cells at 37°C in the presence of the microtubule depolymerizing drug nocodazole. As reported before (Yamamoto *et al*., 1996), most nocodazole-treated wild-type cells arrested in the cell cycle with a large bud, replicated DNA and stable Pds1p in response to the Mad2p checkpoint (Figure 4B). In contrast, *Δmad2* cells failed to arrest at the metaphase to anaphase transition, as indicated by the degradation of nuclear Pds1p. *Δmad2* cells finally arrested at the end of anaphase because of an alternative checkpoint (Bub2p dependent), which is regulated by the movement of the SPB into the bud (Bardin *et al*., 2000; Pereira *et al*., 2000). SPB migration into the bud does not take place when microtubules are depolymerized. Importantly, *spc24-2* cells behaved very similarly to *Δmad2* cells, confirming that the Mad2p checkpoint function is defective. Collectively, these results demonstrate that Spc24p, and possibly also Ndc80p and Spc25p, are important for the Mad2p checkpoint function.

### *Ndc80p, Nuf2p, Spc24p and Spc25p bind to CEN3 DNA, and SPC24 interacts with MCM21*

The chromosome segregation defect of *ndc80-1* (Wigge *et al*., 1998), *spc24-2* and *spc25-7* cells is similar to that of *ndc10-1* cells (Goh and Kilmartin, 1993). Since Ndc10p is a component of the CBF3 kinetochore complex (Lechner and Carbon, 1991), we considered the possibility that the Ndc80p, Nuf2p, Spc24p and Spc25p proteins interact with the kinetochore. This notion was tested by chromatin immunoprecipitation (ChIP) using fully functional, chromosomally tagged *NDC80-6HA*, *NUF2-6HA*, *SPC24-3HA* and *SPC25-3HA* gene fusions. CEN3 DNA was co-immunoprecipitated with Ndc80p-6HA (Figure 5, lane 2), Nuf2p-6HA (lane 4), Spc24p-3HA (lane 6) and Spc25p-3HA (lane 8) by the anti-HA antibodies. These precipitations were found to be specific for CEN3 because CEN3 and control DNAs flanking CEN3 (ChIII-R and ChIII-L) (Ortiz *et al*., 1999) were detected equally in the input (Figure 5, Load, lanes 1, 3, 5 and 7), but only CEN3 was strongly enriched in the immunoprecipitates (Figure 5, IP, lanes 2, 4, 6 and 8). To exclude unspecific CEN3–antibody interactions, a wild-type strain devoid of an HA epitope was processed equally (Figure 5, lanes 9 and 10). In conclusion, the ChIP results suggest that Ndc80p, Nuf2p, Spc24p and Spc25p are components of the kinetochore.

**Table II.** *MCM21* and *SPC24* interact genetically

| Genotype | Growth at the indicated temperature | | | | |
|---|---|---|---|---|---|
| | 23°C | 30°C | 33°C | 35°C | 37°C |
| *Δmcm21* | +++ | +++ | +++ | +++ | +++ |
| *ndc80-1* | +++ | +++ | + | – | – |
| *ndc80-1 Δmcm21* | +++ | +++ | + | – | – |
| *nuf2-61* | +++ | +++ | – | – | – |
| *nuf2-61 Δmcm21* | +++ | +++ | – | – | – |
| *spc24-2* | +++ | +++ | + | – | – |
| *spc24-2 Δmcm21* | – | – | – | – | – |
| *spc24-3* | +++ | +++ | +++ | +++ | – |
| *spc24-3 Δmcm21* | +++ | +++ | +++ | – | – |
| *spc25-4* | +++ | +++ | +++ | + | – |
| *spc25-4 Δmcm21* | +++ | +++ | +++ | + | – |
| *spc25-7* | +++ | +++ | + | – | – |
| *spc25-7 Δmcm21* | +++ | +++ | – | – | – |

Synthetic lethality was determined as described in Materials and methods. –, no growth; +, reduced growth; +++, normal growth on 5-FOA plates. No growth of *spc24-2 Δmcm21* cells at 23 and 30°C indicates synthetic lethality since *spc24-2* or *Δmcm21* cells grew at these temperatures.

This finding is supported by the genetic (Table II) and two-hybrid interactions (Figure 2) of *SPC24* with *MCM21* coding for a subunit of the kinetochore (Ortiz *et al*., 1999). However, attempts to co-immunoprecipitate Mcm21p and Spc24p failed (not shown). This may reflect the fact that both proteins are part of different kinetochore subcomplexes, which may be dissolved upon extraction of the proteins during the immunoprecipitation. Alternatively, the interaction between Spc24p and Mcm21p may be indirect. In summary, *SPC24* interacts genetically with the kinetochore component *MCM21*.

### *Nuf2p co-localizes with the centromere*

To confirm the result of the ChIP analysis, we investigated by immunofluorescence microscopy the localization of Nuf2p, the kinetochore protein Mcm21p (Ortiz *et al*., 1999) and the SPB component Spc98p (Geissler *et al*., 1996) relative to CEN5 DNA. Owing to the clustering of the centromeres over most parts of the cell cycle (Jin *et al*., 2000), kinetochore proteins are observed by immunofluorescence as one or two dots per cell, located close to the nuclear side of the SPB represented by the γ-tubulin complex (Goshima and Yanagida, 2000). Thus, if Nuf2p is a kinetochore component, it should co-localize with CEN5 DNA but behave differently to the γ-tubulin complex protein Spc98p.

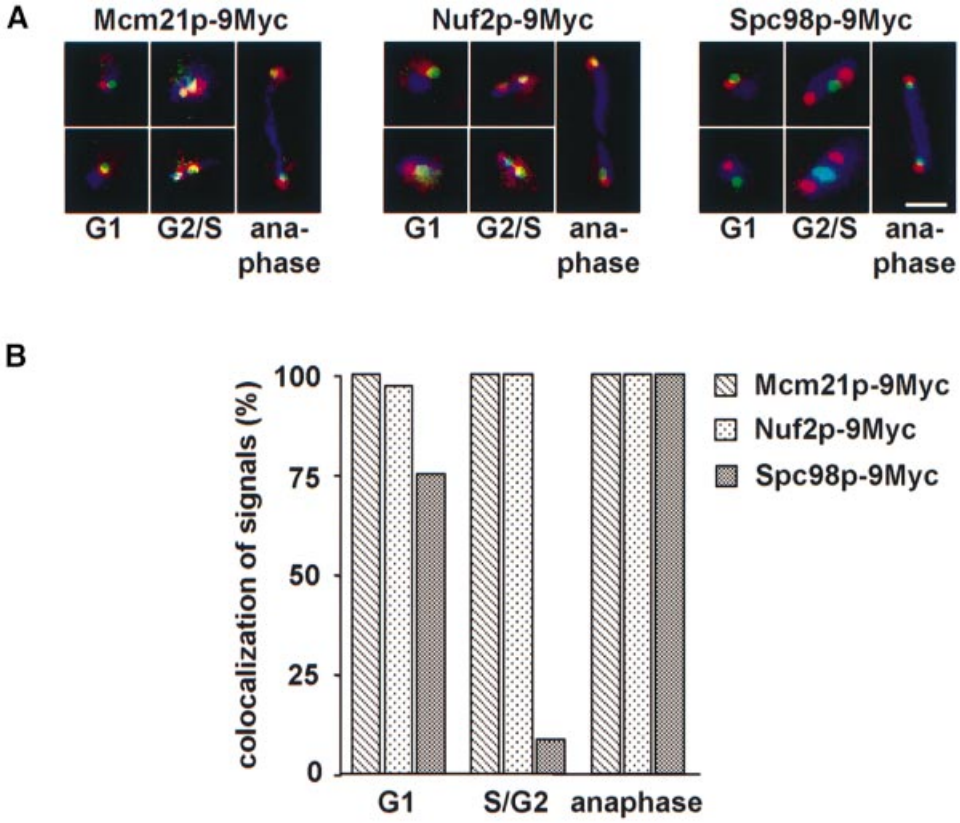


**Fig. 6.** Nuf2p and Mcm21p are located close to the CEN5. (**A**) Localization of Mcm21p-9Myc, Nuf2p-9Myc and Spc98p-9Myc relative to CEN5 DNA. Synchronized cells with GFP-labeled CEN5 DNA carrying *MCM21-9Myc*, *NUF2-9Myc* or *SPC98-9Myc* were fixed and analysed by direct and indirect immunofluorescence for CEN5 DNA (green), Myc-tagged protein (red) and tubulin (blue). Note that the overlap between the green and red signals appears in yellow. Shown are cells in $G_1$ phase (monopolar spindle), $G_2$/S phase (short spindle) and anaphase (long spindle) of the cell cycle. Bar: 5 μm. (**B**) Quantification of (A). Cells ($n$ = 100) in $G_1$, $G_2$/S phase or anaphase of the cell cycle were analysed. Signals were counted as 'co-localized' when the CEN5 signal (green) was <0.4 μm from the red anti-HA dot.

For this study, a strain was constructed in which arrays of TetO binding sites were introduced next to CEN5 DNA (He *et al*., 2000). In this strain, *MCM21*, *NUF2* and *SPC98* were tagged with nine copies of the Myc-epitope. The localization of the three proteins relative to CEN5 was determined in fixed cells. The established kinetochore protein Mcm21p (Figure 6A, Mcm21p-9Myc, red) and Nuf2p (Figure 6A, Nuf2p-9Myc, red) were detected as a dot, which in the vast majority of cells (Figure 6B, >95%) was located <0.4 μm from the green CEN5. A complete overlap between the CEN5 and Mcm21p or Nuf2p signals was only observed in ~30% of the cells. However, a perfect co-localization was not always expected since the CEN5 signal reflects a single centromere, whereas the Nuf2p or Mcm21p signals represent the average of 16 centromeres. Importantly, Nuf2p-9Myc and Mcm21p-9Myc localization relative to CEN5 DNA was independent of whether the cells were in $G_1$, S/$G_2$ or anaphase (Figure 6B). In contrast, in 90% of S/$G_2$ cells the red signal of the SPB component Spc98p-9Myc was clearly distinct (⩾0.4 μm apart) from the green CEN5 (Figure 6A, Spc98p-9Myc, G2/S, and B). However, Spc98p-9Myc was found in most $G_1$ phase (Figure 6A, Spc98p-9Myc, G1, upper panel) and anaphase cells within 0.4 μm of the CEN5 DNA dot (Figure 6A, Spc98p-9Myc, anaphase), indicating that during these stages of the cell cycle kinetochores are clustered very close to the SPB. In ~25% of $G_1$ phase cells, the Spc98p-9Myc and CEN5 signals were clearly different (Figure 6A, Spc98p-9Myc, G1, lower panel). In conclusion, the localization of Nuf2p relative to CEN5 DNA was similar to that of the kinetochore protein Mcm21p, but distinct from the SPB component Spc98p, providing further evidence that Nuf2p is located at the yeast kinetochore.

### *Kinetochore association of Ndc80p and Spc24p is defective in ndc10-1 cells*

In *ndc10-1* cells, the centromere DNA is devoid of most if not all kinetochore proteins (Goh and Kilmartin, 1993; Ortiz *et al*., 1999; Goshima and Yanagida, 2000). Therefore, we would expect that in *ndc10-1* cells Ndc80p and Spc24p are no longer associated with the centromere at the restrictive temperature. *ndc10-1 NDC80-6HA* (Figure 7A, lanes 1, 2, 7 and 8), *ndc10-1 SPC24-3HA* (lanes 3, 4, 9 and 10) and *ndc10-1* cells (control, lanes 5, 6, 11 and 12) were analysed by ChIP. The CEN3 DNA was enriched with Ndc80p-6HA or Spc24p-3HA of *ndc10-1 NDC80-6HA* or *ndc10-1 SPC24-3HA* cells grown at 23°C (lanes 2 and 4, compare Load with IP) but not at 37°C (lanes 8 and 10). No precipitation of CEN3 DNA was observed with the *ndc10-1* control cells at any temperature (lanes 6 and 12).

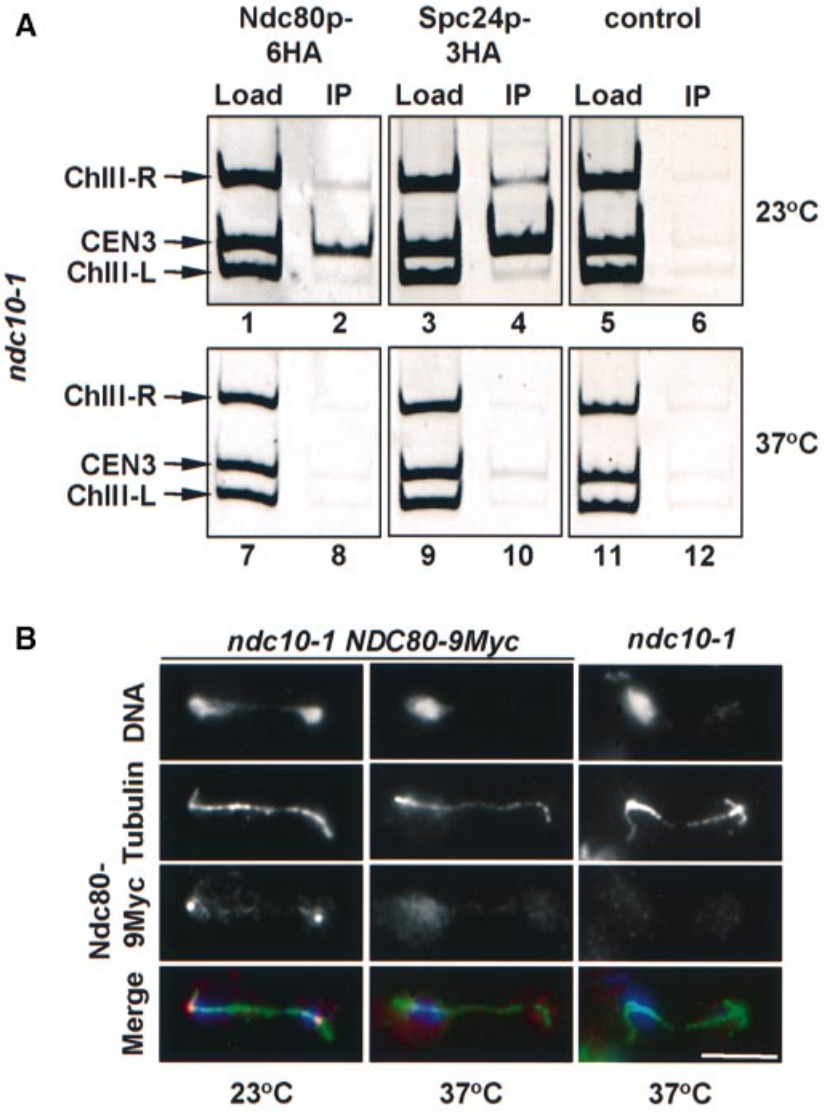


**Fig. 7.** Localization of Ndc80p and Spc24p in *ndc10-1* cells. (**A**) Ndc80p and Spc24p are not associated with the kinetochore in *ndc10-1* cells incubated at the restrictive temperature. Cells of *ndc10-1 NDC80-6HA* (lanes 1, 2, 7 and 8), *ndc10-1 spc24-3HA* (lanes 3, 4, 9 and 10) and *ndc10-1* (control; lanes 5, 6, 11 and 12) grown at 23°C (lanes 1–6) were shifted to 37°C for 4 h (lanes 7–12). CEN3 association of Ndc80p-6HA (lanes 2 and 8) and Spc24p-3HA (lanes 4 and 10) was investigated by ChIP. *ndc10-1* cells were employed as a control for the specificity of the immunoprecipitation (lanes 6 and 12) as well as binding to regions left (ChIII-L) and right (ChIII-R) of CEN3 DNA. Yeast lysates were also tested without precipitation (Load: lanes 1, 3, 5, 7, 9 and 11). (**B**) Cells of *ndc10-1 NDC80-9Myc* and *ndc10-1 NDC80* were shifted from 23 to 37°C for 4 h. Fixed cells were analysed by indirect immunofluorescence using anti-tubulin and anti-Myc antibodies. DNA was stained with DAPI. The bottom panel shows the merged signals of the DNA (blue), tubulin (green) and Ndc80p-9Myc (red) stainings. Bar: 5 μm.

**Fig. 8.** Kinetochores are no longer clustered near SPBs in *spc24-2* cells. (**A**) Mcm21p, Okp1p and Spc24p are associated with CEN3 DNA in *ndc80-1* and *spc24-2* cells. Cells of *ndc80-1* (lanes 1–8) and *spc24-2* (lanes 9–12) were tested for Mcm21p (lanes 1, 2, 9 and 10), Okp1p (lanes 3, 4, 11 and 12) and Spc24p (lanes 5–8) CEN3 DNA localization by ChIP at 23°C (lanes 5 and 6), or after 3 h at 37°C (lanes 1–4 and 7–12) using anti-Mcm21p (lanes 2 and 10), anti-Okp1p (lanes 4 and 12) or anti-Spc24p antibodies (lanes 6 and 8). Binding to regions left (ChIII-L) and right (ChIII-R) of CEN3 was tested as controls. Yeast lysates were assayed without precipitation (Load: lanes 1, 3, 5, 7, 9 and 11). (**B**) Localization of Mcm21p-9Myc in *spc24-2* cells. Cells of *spc24-2 MCM21-9Myc* and *spc24-2* were shifted from 23 to 37°C for 3 h. Fixed cells were analysed by indirect immunofluorescence using anti-Myc and anti-tubulin antibodies. DNA was stained with DAPI. The three signals were merged to compare localization. DAPI is shown in blue, the Mcm21p signal in red and microtubules in green. (**C**) Mcm21p levels remain constant. *spc24-2* (lanes 3 and 6) and *spc24-2 MCM21-9Myc* cells (lanes 1, 2, 4 and 5) were grown at 23°C. One-half of the culture was incubated for 3 h at 37°C (lanes 2, 3, 5 and 6). Cell extracts were separated by SDS–PAGE and transferred to a nitrocellulose membrane. The membrane was stained with Ponceau S (lanes 1–3) to visualize proteins and then processed with anti-Myc antibodies (lanes 4–6). (D and E) Synchronized wild-type, *spc24-2* and *spc25-7* cells with GFP-labelled CEN5 DNA were shifted to 37°C. Cells were processed by anti-tubulin immunofluorescence and then analysed by confocal microscopy. (**D**) Large budded wild-type (panel 1) or *spc24-2* cells (panels 2 and 3) containing an anaphase spindle. Tubulin is shown in red, CEN5 in green and DAPI in blue. (**E**) The position of CEN5 (green dot in cartoon) relative to the spindle pole (intersection of astral and nuclear microtubules) in the mother cell body of cells with an anaphase spindle was determined. Each CEN5 signal was counted separately. At least 100 cells were analysed. (B and D) Bars: 5 μm.

This result was confirmed by the analysis of *ndc10-1 NDC80-9Myc* and *ndc10-1 SPC24-GFP* cells (where GFP is green fluorescent protein) using immunofluorescence microscopy. At 23°C, Ndc80p-9Myc (Figure 7B, *ndc10-1 NDC80-9Myc*) and Spc24p-GFP (not shown) were detected as single dots situated close to the spindle pole. In contrast, in *ndc10-1* cells incubated at 37°C, both Ndc80p-9Myc (Figure 7B, *ndc10-1 NDC80-9Myc*) and Spc24p-GFP (not shown) localized diffusely in the nucleus. No signal was detected with the anti-Myc antibody when *ndc10-1* cells were used (Figure 7B, panel *ndc10-1*), indicating that the Ndc80p-9Myc signal in *ndc10-1 NDC80-9Myc* cells was specific. Therefore, both ChIP and immunofluorescence microscopy indicate that the localization of Ndc80p and Spc24p with the kinetochore is dependent on Ndc10p.

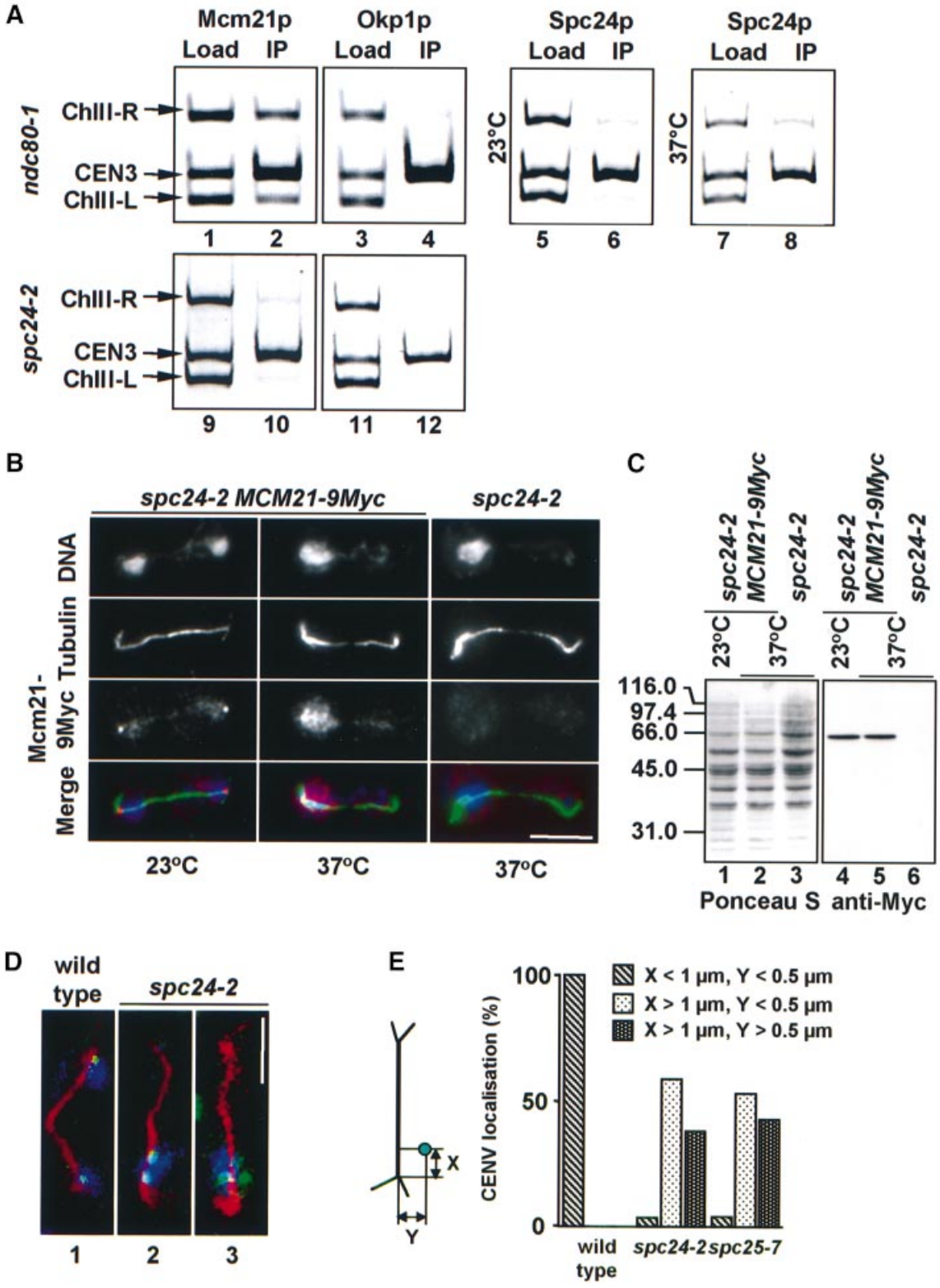

### *Kinetochores are no longer clustered in spc24-2 and spc25-7 cells*

We investigated by ChIP whether mutations in *NDC80* or *SPC24* affect the overall structure of the yeast kinetochore. When *ndc80-1* (Figure 8A, lanes 1–8) or *spc24-2* cells (lanes 9–12) were shifted to 37°C, the core kinetochore proteins Ctf13p, Ctf19p (data not shown), Mcm21p (lanes 2 and 10) and Okp1p (lanes 4 and 12) as well as Spc24p (lane 8) were still associated with CEN3 DNA. The relative Spc24p signals (ratio of load/IP) at 23°C (lanes 5 and 6) and 37°C (lanes 7 and 8) were about the same (0.9 versus 0.8), suggesting that Spc24p localization with CEN3 was hardly affected in *ndc80-1* cells. When taken together, these results suggest that the kinetochore is still partially intact in *ndc80-1* and *spc24-2* cells.

*spc24-2* and *spc25-7* cells may fail to segregate the chromosomes because the kinetochore is defective in bipolar attachment to microtubules, binding to microtubules or clustering at the SPB. To elucidate the kinetochore defect of *spc24-2* and *spc25-7* cells, we investigated the localization of the kinetochore protein Mcm21p. The Mcm21p-9Myc signal was situated 'dot-like' close to spindle poles, indicative of centromere clustering, in *spc24-2* cells at 23°C (Figure 8B, *spc24-2 MCM21-9Myc*). When *spc24-2* cells were shifted to 37°C, however, the Mcm21p-9Myc staining was no longer clustered. Instead, the Mcm21p-9Myc signal was dispersed within the DAPI staining region in the mother cell body (Figure 8B, *spc24-2 MCM21-9Myc*). The Mcm21p-9Myc signal was found to be specific since only a faint background signal was observed when *spc24-2* cells were incubated with the anti-Myc antibodies (Figure 8B, *spc24-2*). Furthermore, we established by immunoblotting that the dispersed Mcm21p-9Myc signal of *spc24-2* cells at 37°C was not the result of increased Mcm21p levels (Figure 8C, compare lanes 4 and 5).

The failure of kinetochores to cluster close to the SPB was confirmed by using *spc24-2* and *spc25-7* cells in which TetO binding sites were introduced adjacent to CEN5. In anaphase wild-type cells at 37°C, CEN5 was always found close to the spindle poles (Figure 8D, panel 1, and 8E). In contrast, in 98% of the *spc24-2* and *spc25-7* cells, CEN5 was located in the nucleoplasm of the mother cell body either close to (Figure 8D, panel 2) or >0.5 μm away from (panel 3) microtubules, but not near the spindle poles. Furthermore, >50%, approximately, of the CEN5 signals of *spc24-2* and *spc25-7* cells appeared as two discrete dots. This result is consistent with our previous finding (Figure 4) indicating that *spc24-2* cells degrade Pds1p and therefore probably also the cohesin Scc1p, the latter being responsible for sister chromatid cohesion in metaphase (Uhlmann *et al*., 2000). In conclusion, although the core kinetochore structure is at least partially intact in *spc24-2* cells, the kinetochores fail to cluster close to the spindle poles. Since microtubuli have been described to be important for centromere clustering (Jin *et al*., 2000), one explanation for the clustering defect is a lack of microtubule attachment.

## Discussion

Ndc80p, Nuf2p, Spc24p and Spc25p belong to a group of proteins that have been co-purified with the budding yeast spindle and localize at or adjacent to the SPB (Rout and Kilmartin, 1990; Wigge *et al*., 1998). In this study we show that the four proteins interact, a conclusion that is based on the co-purification of Ndc80p and Spc24p with Spc25p–ProA, the co-immunoprecipitation of the four proteins, and two-hybrid and genetic interactions of *NDC80*, *NUF2*, *SPC24* and *SPC25*. An interaction of Ndc80p and Nuf2p is also consistent with the co-localization of both proteins observed by indirect immunofluorescence (Osborne *et al*., 1994).

Ndc80p, Spc24p and Spc25p have been localized by immunoelectron microscopy close to the nuclear inner plaque of the SPB (Wigge *et al*., 1998). After the observation that centromeres are clustered in the vicinity of the SPB (Goh and Kilmartin, 1993; Hyland *et al*., 1999; Goshima and Yanagida, 2000; He *et al*., 2000; Jin *et al*., 2000; Tanaka *et al*., 2000), it became feasible that the cellular localization of Ndc80p, Spc24p and Spc25p reflects clustered centromeres. Here we provide evidence that Ndc80p, Spc24p, Spc25p and Nuf2p are indeed associated with the kinetochore. First, ChIP experiments clearly demonstrate that the four proteins are localized to the centromere DNA in an Ndc10p-dependent manner. Secondly, immunofluorescence microscopy detects Nuf2p close to CEN5 DNA. Thirdly, *MCM21* interacts genetically with *SPC24*. Finally, the phenotype of conditional lethal mutants (discussed below) is consistent with a kinetochore function of Ndc80p, Spc24p and Spc25p. Our conclusion is supported further by the conditional synthetic lethal effect of *ndc80-1* and *Δctf19* [*CTF19* codes for a kinetochore protein (Hyland *et al*., 1999)] and by the finding that the human homologue of Ndc80p, HEC1, localizes to the centromere (Chen *et al*., 1997).

Kinetochores provide the attachment sites for spindle microtubules, are required for centromere DNA clustering at the SPB, regulate progress through mitosis upon spindle attachment, possibly sense bipolarity and are a prerequisite for cohesin complex formation in the centromere region of the chromosome (Pidoux and Allshire, 2000). A complete disruption of the centromere, as in *ndc10-1* cells, is likely to eliminate all of these functions, but this is not the case in *ndc80-1* and *spc24-2* cells because these mutants maintain partially assembled kinetochores, as judged from ChIP experiments. Therefore, we propose that the phenotypes of *ndc80-1*, *spc24-2* and *spc25-7* cells indicate specific functions of the encoded proteins at the kinetochore.

The phenotypes of *ndc80-1* (Wigge *et al*., 1998), *spc24-2* and *spc25-2* cells (this study) were remarkably similar. All the mutant cells formed an anaphase spindle of wild-type morphology, which failed to segregate the duplicated chromosomes. The reason for the chromosome segregation defect is not fully understood. Our data reveal that kinetochores are no longer clustered at SPBs in *spc24-2* and *spc25-7* cells. This indicates that either the kinetochores fail to bind to microtubules or that a direct interaction between the kinetochore and the SPB is defective. Notably, kinetochores of *spc24-2* and *spc25-7* cells were often (in ~55% of cases) found close to the anaphase spindle, suggesting that some kinetochores may have microtubule binding activity. In any case, microtubule binding of *spc24-2* and *spc25-7* kinetochores must be impaired, since ~45% of the centromeres were located >0.5 μm from microtubules.

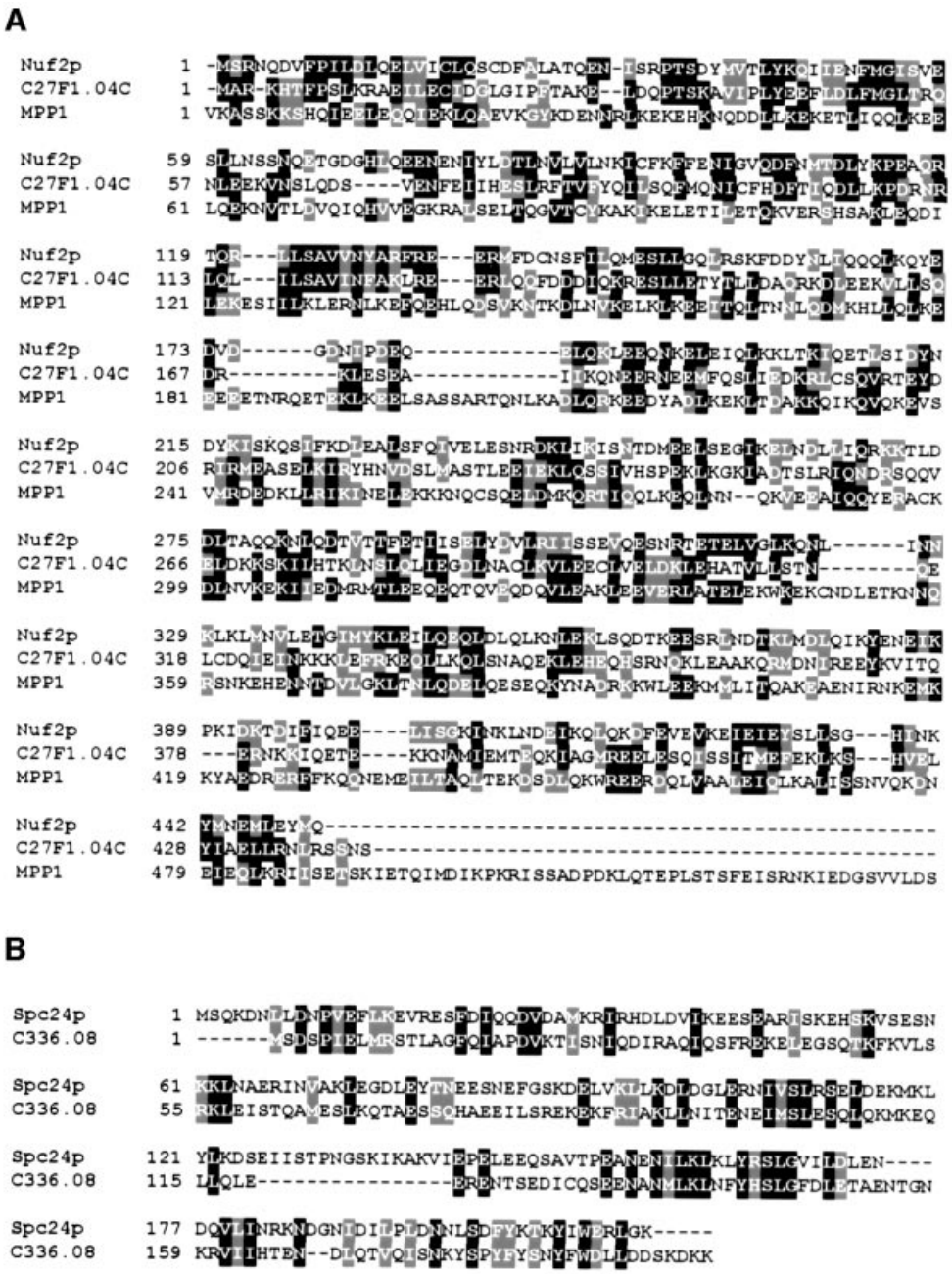


**Fig. 9.** Alignment of homologues of Nuf2p and Spc24p (program Clustal_X; Thompson *et al*., 1997). Homologous proteins were identified in a BLAST search (program WU-blastp; database, swall; matrix, blosum62; Altschul and Gish, 1996) using the protein sequence of Nuf2p and Spc24p. (**A**) The *S.pombe* homologue of Nuf2p, C27F1.04C [P(N) of $1.1 \times 10^{-27}$; high score of 318], is a hypothetical 51.9 kDa protein. The human MPP1 protein is homologue of Nuf2p [P(N) of $1.3 \times 10^{-10}$; high score of 183]. Note that MPP1 is a protein of 225 kDa (Fritzler *et al*., 2000). (**B**) The *S.pombe* homologue of Spc24p, C336.08, is a hypothetical 23.0 kDa protein [P(N) of $2.1 \times 10^{-10}$; high score of 148]. Identical amino acids are highlighted in black and similar amino acids in grey.

It is possible that the binding of Ndc80p, Spc24p and Spc25p to SPB components assists chromosome segregation during anaphase B. In favour of this model is the clustering of centromeres along the nuclear face of the SPB (Goshima and Yanagida, 2000; this study), the co-purification of Ndc80p, Spc24p and Spc25p with the SPB, whereas other core kinetochore proteins like Ndc10p were not identified in this preparation (Wigge *et al*., 1998), and the finding that microtubule depolymerization affects centromere clustering only moderately (Jin *et al*., 2000). Notably, Spc24p and Spc25p interact with core SPB components, as seen in the yeast two-hybrid system (Newman *et al*., 2000; C.Janke, unpublished), although as yet we have been unable to confirm these interactions by co-immunoprecipitation. However, an argument against a prolonged interaction of kinetochore components and the SPB is the rapid change in distance between the centromere and the SPB, as seen by time-lapse experiments using the central SPB component Spc42p and CEN5 DNA as markers (He *et al*., 2000; Tanaka *et al*., 2000).

Some of these changes may be attributed to the stretching of Spc110p, a filamentous SPB component that connects the γ-tubulin complex to the central Spc42p layer (Kilmartin *et al*., 1993; Knop and Schiebel, 1997).

A defect in spindle–kinetochore interaction should trigger the Mad2p checkpoint, which arrests cells in metaphase with unseparated sister chromatids and a short spindle (Hwang *et al*., 1998). Consistently, cells of *ctf13-30*, *Δctf19* and *mtw1-1* (Spencer and Hieter, 1992; Hyland *et al*., 1999; Goshima and Yanagida, 2000) stop cell cycle progression at the metaphase to anaphase transition in a Mad2p-dependent manner (Wang and Burke, 1995). In contrast, *spc24-2* cells were only slightly delayed in anaphase entry despite their complete failure to segregate the chromosomes, suggesting a checkpoint defect. This notion is further supported by the observation that *spc24-2* cells at 37°C did not arrest at the metaphase to anaphase transition when microtubules were depolymerized.

The kinetochore of mammalian cells provides an essential scaffold for the binding and function of the checkpoint proteins BUB1 (Taylor and McKeon, 1997), BUB3 (Taylor *et al*., 1998), MAD2 (Chen *et al*., 1996) and BUBR1 (Chan *et al*., 1999). Centromere proteins such as CENP-E have been found to interact with BUBR1 and are essential for checkpoint control (Abrieu *et al*., 2000). Similarly, Ndc80p, Spc24p and Spc25p may provide an essential scaffold that allows Mad2p checkpoint components to assemble at the kinetochore and which may be crucial for the sensing of microtubule attachment defects. In this respect, it is interesting that a two-hybrid interaction has been reported for Mad1p and Spc25p (Newman *et al*., 2000).

The phenotype of *nuf2-61* cells was less informative. They arrested in the cell cycle with a short metaphase-like spindle (Osborne *et al*., 1994) in response to the Mad2p checkpoint (E.Schiebel, unpublished). This arrest phenotype indicates that *nuf2-61* cells are still checkpoint proficient. Analysis of additional *nuf2(ts)* alleles will reveal whether *NUF2* has the same or merely an overlapping function with *NDC80*, *SPC24* and *SPC25*.

Homologues of Ndc80p and Nuf2p have been identified from fission yeast to mammalian cells. Ndc80p shares 30% identity with mammalian HEC1 (Wigge *et al*., 1998). A similar function of the HEC1 protein and Ndc80p is suggested by the finding that both proteins associate with the kinetochore and are important for chromosome segregation (Chen *et al*., 1997; Wigge *et al*., 1998). Importantly, deletion of the essential yeast *NDC80* is fully complemented by the human HEC1, demonstrating the close functional relationship of both genes (Zheng *et al*., 1999). Databank searches revealed that the human MPP1 protein is 25% identical to Nuf2p over 280 amino acids (Figure 9A). MPP1 has been identified as an M-phase nuclear phosphoprotein recognized by the MPM2 monoclonal antibody (Westendorf *et al*., 1994; Fritzler *et al*., 2000). In addition, *Schizosaccharomyces pombe* proteins of unknown function with 25% identity to Nuf2p (Figure 9A) or Spc24p (Figure 9B) are present in the database. When taken together, it is likely that homologues of Ndc80p, Nuf2p and Spc24p interact in other organisms. These proteins may also be associated with kinetochores and function in the attachment of kinetochores to microtubules and in checkpoint control.

## Materials and methods

### Growth media, strain and plasmid construction, and two-hybrid analysis

Basic yeast methods and growth media were as described previously (Sherman, 1991). Yeast strains were grown in yeast extract, peptone and dextrose medium containing 100 mg/l adenine (YPAD medium). Synthetic complete (SC) medium was used to select for plasmids in yeast. Yeast strains and plasmids are described in Table III. Yeast strains were constructed using PCR-amplified cassettes (Knop *et al*., 1999). To tag the CEN5 DNA, plasmid pXH136 (He *et al*., 2000) was restricted with *Bam*HI and integrated next to CEN5 by homologous recombination. TetR–GFP of plasmid pXH123 (Michaelis *et al*., 1997) or pCJ092 was integrated into the *LEU2* or *ADE2* locus, respectively. For the construction of temperature-sensitive alleles, *SPC24* and *SPC25* were mutagenized by PCR and conditional lethal alleles were selected (Geissler *et al*., 1996). Two-hybrid interactions were analysed as described previously (Pereira *et al*., 1999).

### Analysis of conditional lethal spc24 and spc25 mutants

Yeast cells were incubated at 23°C for 2.5 h with α-factor (1 μg/ml for *Δsst1* and 10 μg/ml for *SST1* cells) to arrest cells in $G_1$ phase of the cell cycle. α-factor was removed by washing the cells with pre-warmed (37°C) YPAD medium ($t = 0$). Cells were then incubated in YPAD at 37°C. At the times indicated, cells were fixed with formaldehyde for indirect immunofluorescence, the budding index was determined after fixation in 70% ethanol and the DNA content was analysed by flow cytometry (Hutter and Eipel, 1979).

### High gene dosage suppression and synthetic lethality

*ndc80-1*, *ndc80-2*, *nuf2-61*, *spc24-2*, *spc24-3*, *spc25-4* and *spc25-7* cells were transformed with *NDC80*, *NUF2*, *SPC24*, *SPC25* and *SPC98* on the 2 μm, high-copy-number plasmid pRS426 and with pRS426. Transformants were tested for 3–4 days for growth at 23, 30, 33, 35 and 37°C. To test for synthetic lethality, *ndc80-1*, *ndc80-2*, *nuf2-61*, *spc24-2*, *spc24-3*, *spc25-4* and *spc25-7* cells were complemented with the defective gene on pRS316. *MCM21* was disrupted using a PCR-based cassette containing the *TRP1* marker from *Kluyveromyces lactis* (*klTRP1*) (Knop *et al*., 1999). Disruption was confirmed by colony PCR. *Δmcm21* cells were grown on 5-fluoroorotic acid (5-FOA) plates at 23, 30, 33, 35 and 37°C for 3 days.

### Purification of Spc25p–ProA

*SPC25–ProA* cells and *SPC25* control cells were grown to mid-logarithmic phase in YPAD medium at 30°C. The cell pellet (5 g each) was resuspended in IP-buffer (50 mM Tris–HCl pH 7.6, 10 mM EDTA, 1 mM EGTA, 100 mM NaCl, 5% glycerol) containing protease inhibitors [cØmplete™ (from Boehringer Mannheim), 1 mM phenylmethylsulfonyl fluoride, 4 μg/ml pepstatin, 2.5 mM benzamidine]. After cell breakage, 1% Triton X-100 was added and cells were incubated at 4°C for 45 min. The cleared lysate (10 000 *g* for 15 min at 4°C) was incubated with magnetic beads coated with rabbit IgGs (1.5 h). The beads were washed with IP-buffer, 1% Triton X-100 and IP-buffer alone. Proteins were eluted from the beads by heating the beads in sample buffer (Knop *et al*., 1999) for 15 min at 65°C. The protein samples were resolved by a 6–18% SDS–PAGE gradient gel and stained with Coomassie Blue. Selected protein bands were analysed by MALDI analysis (Shevchenko *et al*., 1996).

### ChIP

ChIPs of yeast cells were performed as described previously (Hecht and Grunstein, 1999). The anti-HA antibody (3F10) was used for the immunoprecipitation of HA-tagged proteins at a concentration of 0.6 ng/ml. The primers used to amplify the CEN DNA and the non-target DNAs are described (Ortiz *et al*., 1999) as CENwt, III-L and III-R. The ChIP PCR reactions contained 0.025% of the chromatin preparation for the input and 1.8% of the chromatin preparation for the immunoprecipitations.

### Immunological techniques and microscopy

Anti-N-Nuf2p, anti-C-Nuf2p and anti-Spc24p antibodies were raised in rabbits against purified glutathione *S*-transferase (GST) fusion proteins.

**Table III.** Yeast strains and plasmids

| Name | Genotype | Reference |
|---|---|---|
| CJY016 | *MAT***a** *ura3-52 lys2-801 ade2-101 trp1Δ63 his3Δ200 leu2Δ1 SPC24-3HA::kanMX6* | this study |
| CJY045 | *MAT***a** *ura3-52 lys2-801 ade2-101 trp1Δ63 his3Δ200 Δspc25::HIS3MX4 leu2Δ1::pCJ020* | this study |
| CJY048 | *MAT***a** *ura3-52 lys2-801 ade2-101 trp1Δ63 his3Δ200 Δspc25::HIS3MX4 leu2Δ1::pCJ023* | this study |
| CJY083 | *MAT***a** *Δspc24::kanMX6 ura3-52 lys2-801 ade2-101 trp1Δ63 his3Δ200 leu2Δ1::pCJ062* | this study |
| CJY084 | *MAT***a** *Δspc24::kanMX6 ura3-52 lys2-801 ade2-101 trp1Δ63 his3Δ200 leu2Δ1::pCJ063* | this study |
| CJY092 | *MAT***a** *ura3-52 lys2-801 ade2-101 trp1Δ63 his3Δ200 leu2Δ1 NDC80-6HA::klTRP1* | this study |
| CJY132 | *MAT***a** *ura3-52 lys2-801 ade2-101 trp1Δ63 his3Δ200 Δspc25::HIS3MX4 leu2Δ1::pCJ023 Δsst1::URA3 PDS1-6HA::klTRP1* | this study |
| CJY138 | *MAT***a** *ura3-52 lys2-801 ade2-101 trp1Δ63 his3Δ200 leu2Δ1 Δsst1::URA3 PDS1-6HA::klTRP1* | this study |
| CJY176 | *MAT***a** *Δspc24::kanMX6 ura3-52 lys2-801 ade2-101 trp1Δ63 his3Δ200 leu2Δ1::pCJ062 Δsst1::URA3 PDS1-6HA::klTRP1* | this study |
| CJY184 | *MAT***a** *ura3-52::pXH136 lys2-801 trp1Δ63 his3Δ200 leu2Δ1::pXH123* | this study |
| CJY189 | *MAT***a** *ura3-52::pXH136 lys2-801 trp1Δ63 his3Δ200 leu2Δ1::pXH123 NUF2-9Myc::klTRP1* | this study |
| CJY191 | *MAT***a** *ura3-52 lys2-801 ade2-101 trp1Δ63 his3Δ200 Δspc25::HIS3MX4 leu2Δ1::pCJ023 Δsst1::URA3 MCM21-9Myc::klTRP1* | this study |
| CJY193 | *MAT***a** *Δspc24::kanMX6 ura3-52 lys2-801 ade2-101 trp1Δ63 his3Δ200 leu2Δ1::pCJ062 Δsst1::URA3 MCM21-9Myc::klTRP1* | this study |
| CJY195 | *MAT***a** *ura3-52::pXH136 lys2-801 trp1Δ63 his3Δ200 leu2Δ1::pXH123 SPC98-9Myc::klTRP1* | this study |
| CJY197 | *MAT***a** *ura3-52::pXH136 lys2-801 trp1Δ63 his3Δ200 leu2Δ1::pXH123 MCM21-9Myc::klTRP1* | this study |
| CJY231 | *MAT***a** *ura3-52::pXH136 lys2-801 ade2-101::pCJ092 trp1Δ63 his3Δ200 Δspc25::HIS3MX4 leu2Δ1::pCJ023* | this study |
| CJY232 | *MAT***a** *Δspc24::kanMX6 ura3-52::pXH136 lys2-801 ade2-101::pCJ092 trp1Δ63 his3Δ200 leu2Δ1::pCJ062* | this study |
| CJY233 | *MAT***a** *Δmad2::kanMX6 ura3-52 lys2-801 ade2-101 trp1Δ63 his3Δ200 leu2Δ1 PDS1-6HA::klTRP1* | this study |
| ESM480 | *MAT***a** *ura3-52 lys2-801 ade2-101 trp1Δ63 his3Δ200 leu2Δ1 SPC25-3HA::kanMX6* | this study |
| ESM493 | *MAT***a** *ura3-52 lys2-801 ade2-101 trp1Δ63 his3Δ200 leu2Δ1 SPC25-ProA::kanMX6* | this study |
| ESM835 | *MAT***a** *ura3-52 lys2-801 ade2-101 trp1Δ63 his3Δ200 leu2Δ1 Δsst1 NUF2-6HA::klTRP1* | this study |
| ESM965 | *MAT***a** *Δduo1::kanMX6 ura3-52 lys2-801 ade2-101 trp1Δ63 his3Δ200 leu2::pSM808 PDS1-6HA-klTRP1* | this study |
| ESM1286 | *MAT***a** *ura3-52 lys2-801 trp1Δ63 his3Δ200 leu2Δ1 ndc10-1 NUF2-GFP::kanMX6* | this study |
| ESM1287 | *MAT***a** *ura3-52 lys2-801 trp1Δ63 his3Δ200 leu2Δ1 ndc10-1 SPC24-GFP::kanMX6* | this study |
| ESM1290 | *MAT***a** *ura3-52 lys2-801 trp1Δ63 his3Δ200 leu2Δ1 ndc10-1 NDC80-6HA::klTRP1* | this study |
| ESM1291 | *MAT***a** *ura3-52 lys2-801 trp1Δ63 his3Δ200 leu2Δ1 ndc10-1 NDC80-9Myc::klTRP1* | this study |
| ESM1292 | *MAT***a** *ura3-52 lys2-801 trp1Δ63 his3Δ200 leu2Δ1 ndc10-1 SPC24-6HA::klTRP1* | this study |
| JK421 | *MAT***a** *ura3-52 lys2-801 trp1Δ63 his3Δ200 leu2Δ1 ndc10-1* | Goh and Kilmartin (1993) |
| ndc80-1 | *MAT***a** *ura3-52 lys2-801 trp1Δ63 his3Δ200 leu2Δ1 ndc80-1* | Wigge *et al.* (1998) |
| ndc80-2 | *MAT***a** *ura3-52 lys2-801 trp1Δ63 his3Δ200 leu2Δ1 ndc80-2* | Wigge *et al.* (1998) |
| PSY455 | *MAT***a** *leu2-3, 112 ura3-52 trp1Δ1 nuf2-61* | Osborne *et al.* (1994) |
| SGY37 | *MAT***a** *ura3-52::URA3-lexA-op-LacZ trp1Δ63 his3Δ200 leu2Δ1* | Geissler *et al.* (1996) |
| YPH499 | *MAT***a** *ura3-52 lys2-801 ade2-101 trp1Δ63 his3Δ200 leu2Δ1* | Sikorski and Hieter (1989) |
| YPH500 | *MAT*α *ura3-52 lys2-801 ade2-101 trp1Δ63 his3Δ200 leu2Δ1* | Sikorski and Hieter (1989) |
| pACT2 | 2 μm, *LEU2*-based vector carrying the *GAL4* activator domain | Durfee *et al.* (1993) |
| pCJ020 | *spc25-4* in pRS305 | this study |
| pCJ023 | *spc25-7* in pRS305 | this study |
| pCJ062 | *spc24-2* in pRS305 | this study |
| pCJ063 | *spc24-3* in pRS305 | this study |
| pCJ092 | *tetR-GFP* in pRS402 | this study |
| pEG202 | 2 μm, *HIS3*-based vector carrying the *LexA* DNA-binding domain | Gyuris *et al.* (1993) |
| pJO527 | *MCM21* in pACT2 | Ortiz *et al.* (1999) |
| pRS305 | *LEU2*-based integration vector | Sikorski and Hieter (1989) |
| pRS316 | *CEN6, URA3*-based yeast–*Escherichia coli* shuttle vector | Sikorski and Hieter (1989) |
| pRS426 | 2 μm, *URA3*-based yeast–*Escherichia coli* shuttle vector | Christianson *et al*. (1992) |
| pSM149 | *NUF2* (codon 1–177) in pGEX-4T-3 | this study |
| pSM150 | *NUF2* (codon 244–452) in pGEX-4T-3 | this study |
| pSM539 | *SPC25* in pACT2 | this study |
| pSM540 | *SPC25* in pEG202 | this study |
| pSM542 | *SPC24* in pACT2 | this study |
| pSM543 | *SPC24* in pEG202 | this study |
| pSM557 | *SPC34* in pACT2 | this study |
| pSM558 | *SPC34* in pEG202 | this study |
| pSM561 | *SPC25* in pRS316 | this study |
| pSM562 | *SPC24* in pRS316 | this study |
| pSM702 | *SPC24* in pGEX-5X-1 | this study |
| pSM742 | *NUF2* in pRS426 | this study |
| pSM744 | *SPC98* in pRS426 | this study |
| pSM746 | *SPC24* in pRS426 | this study |
| pSM747 | *SPC25* in pRS426 | this study |
| pSM758 | *NUF2* (codon 1–177) in pACT2 | this study |
| pSM759 | *NUF2* (codon 244–452) in pACT2 | this study |
| pSM764 | *NUF2* (codon 1–177) in pEG202 | this study |
| pSM765 | *NUF2* (codon 244–452) in pEG202 | this study |
| pSM778 | *NDC80* in pACT2 | this study |
| pSM779 | *NDC80* in pEG202 | this study |
| pSM791 | *NDC80* in pRS426 | this study |
| pSM808 | *duo1-2* in pRS305 | this study |
| pXH123 | *tetR–GFP* in a *LEU2*-based integration vector | Michaelis *et al.* (1997) |
| pXH136 | 112× tetO in pRS306-based integration vector containing recombination signal for chromosome V | He *et al.* (2000) |

Antibodies were affinity purified using GST fusion proteins coupled to CNBr–Sepharose (Pharmacia).

The polyclonal rabbit anti-Mcm21p, anti-Okp1p (Ortiz *et al*., 1999), anti-Tub4p (Spang *et al*., 1996), anti-Spc72p (Knop and Schiebel, 1998) and anti-Spc110p antibodies (Knop and Schiebel, 1997) have been described. Rabbit polyclonal or mouse monoclonal anti-β-tubulin antibody (Wa3) was used to detect Tub2p (Spang *et al*., 1996). Mouse monoclonal anti-HA antibodies (12CA5 or 3F10) or anti-Myc antibody (9E10) were obtained from Hiss Diagnostics, Boehringer Mannheim or Boehringer Ingelheim. Secondary antibodies used were goat anti-mouse and goat anti-rabbit antibodies coupled to Cy2, Cy3 or 6-((7-amino-4-methylcoumarin-3-acetyl)amino)hexanoic acid (AMCA), or goat anti-rabbit antibodies coupled to horseradish peroxidase (Jackson ImmunoResearch Laboratories). Immunofluorescence of formaldehyde-fixed yeast cells was performed with 40 min fixation time. Samples were analysed using either a Zeiss Axiophot microscope or a Leica SP2 LCS confocal microscope.

Immunoprecipitation of Ndc80p-6HA and Spc25p-6HA proteins was performed as described (Pereira *et al*., 1998) using IP-buffer (see above). The anti-HA antibodies were cross-linked to protein A–Sepharose beads (Pereira *et al*., 1999). Proteins were separated by SDS–PAGE with broad range molecular weight markers from Bio-Rad. Immunoreactions were visualized by an enhanced chemiluminescence (ECL) kit from Amersham.

## Acknowledgements

The work of E.S. was supported by the HFSP (RG0319/1999) and the Cancer Research Campaign. We thank K.Nasmyth, J.Kilmartin, P.Silver and P.Sorger for antibodies, plasmids or yeast strains. We are grateful to G.Pereira and J.Grindlay for carefully reading the manuscript, and to R.H.Wilson and K.Vass for advice on sequence analysis.

## References

Abrieu,A., Kahana,J.A., Wood,K.W. and Cleveland,D.W. (2000) CENP-E as an essential component of the mitotic checkpoint *in vitro*. *Cell*, **102**, 817–826.

Altschul,S.F. and Gish,W. (1996) Local alignment statistics. *Methods Enzymol.*, **266**, 460–480.

Bardin,A.J., Visintin,R. and Amon,A. (2000) A mechanism for coupling exit from mitosis to partitioning of the nucleus. *Cell*, **102**, 21–31.

Chan,G.K., Jablonski,S.A., Sudakin,V., Hittle,J.C. and Yen,T.J. (1999) Human BUBR1 is a mitotic checkpoint kinase that monitors CENP-E functions at kinetochores and binds the cyclosome/APC. *J. Cell Biol.*, **146**, 941–954.

Chen,R.H., Waters,J.C., Salmon,E.D. and Murray,A.W. (1996) Association of spindle assembly checkpoint component XMAD2 with unattached kinetochores. *Science*, **274**, 242–246.

Chen,Y., Riley,D.J., Chen,P.-L. and Lee,W.-H. (1997) HEC, a novel nuclear protein rich in leucine heptad repeats specifically involved in mitosis. *Mol. Cell. Biol.*, **17**, 6049–6056.

Cho,R.J., Fromont-Racine,M., Wodicka,L., Feierbach,B., Stearns,T., Legrain,P., Lockhart,D.J. and Davis,R.W. (1998) Parallel analysis of genetic selections using whole genome oligonucleotide arrays. *Proc. Natl Acad. Sci. USA*, **95**, 3752–3757.

Christianson,T.W., Sikorski,R.S., Dante,M., Shero,J.H. and Hieter,P. (1992) Multifunctional yeast high-copy-number shuttle vectors. *Gene*, **110**, 119–122.

Donaldson,D. and Kilmartin,V. (1996) Spc42p: a phosphorylated component of the *S. cerevisiae* spindle pole body (SPB) with an essential function during SPB duplication. *J. Cell Biol.*, **132**, 887–901.

Durfee,T., Becherer,K., Chen,P.L., Yeh,S.H., Yang,Y., Kilburn,A.E., Lee,W.H. and Elledge,S.J. (1993) The retinoblastoma protein associates with the protein phosphatase type 1 catalytic subunit. *Genes Dev.*, **7**, 555–569.

Fitzgerald-Hayes,M., Clarke,L. and Carbon,J. (1982) Nucleotide sequence comparisons and functional analysis of yeast centromere DNAs. *Cell*, **29**, 235–244.

Fritzler,M.J., Kerfoot,S.M., Feasby,T.E., Zochodne,D.W., Westendorf,J.M., Dalmau,J.O. and Chan,E.K. (2000) Autoantibodies from patients with idiopathic ataxia bind to M-phase phosphoprotein-1 (MPP1). *J. Invest. Med.*, **48**, 28–39.

Geissler,S., Pereira,G., Spang,A., Knop,M., Souès,S., Kilmartin,J. and Schiebel,E. (1996) The spindle pole body component Spc98p interacts with the γ-tubulin-like Tub4p of *Saccharomyces cerevisiae* at the sites of microtubule attachment. *EMBO J.*, **15**, 3899–3911.

Goh,P.Y. and Kilmartin,J.V. (1993) *NDC10*: a gene involved in chromosome segregation in *Saccharomyces cerevisiae*. *J. Cell Biol.*, **121**, 503–512.

Goshima,G. and Yanagida,M. (2000) Establishing biorientation occurs with precocious separation of the sister kinetochores, but not the arms, in the early spindle of budding yeast. *Cell*, **100**, 619–633.

Gyuris,J., Golemis,E., Chertkov,H. and Brent,R. (1993) Cdi1, a human $G_1$ and S phase protein phosphatase that associates with Cdk2. *Cell*, **75**, 791–803.

He,X., Asthana,S. and Sorger,P.K. (2000) Transient sister chromatid separation and elastic deformation of chromosomes during mitosis in budding yeast. *Cell*, **101**, 763–775.

Hecht,A. and Grunstein,M. (1999) Mapping DNA interaction sites of chromosomal proteins using immunoprecipitation and polymerase chain reaction. *Methods Enzymol.*, **304**, 399–414.

Hofmann,C., Cheeseman,I.M., Goode,B.L., McDonald,K.L., Barnes,G. and Drubin,D.G. (1998) *Saccharomyces cerevisiae* Duo1p and Dam1p, novel proteins involved in mitotic spindle function. *J. Cell Biol.*, **143**, 1029–1040.

Hutter,K.J. and Eipel,H.E. (1979) Microbial determination by flow cytometry. *J. Gen. Microbiol.*, **113**, 369–375.

Hwang,L.H., Lau,L.F., Smith,D.L., Mistrot,C.A., Hardwick,K.G., Hwang,E.S., Amon,A. and Murray,A.W. (1998) Budding yeast Cdc20: a target of the spindle checkpoint. *Science*, **279**, 1041–1044.

Hyland,K.M., Kingsbury,J., Koshland,D. and Hieter,P. (1999) Ctf10p: a novel kinetochore protein in *Saccharomyces cerevisiae* and a potential link between the kinetochore and mitotic spindle. *J. Cell Biol.*, **145**, 15–28.

Jin,Q.-W., Fuchs,J. and Loidl,J. (2000) Centromere clustering is a major determinant of yeast interphase nuclear organization. *J. Cell Sci.*, **113**, 1903–1912.

Kilmartin,J.V., Dyos,S.L., Kershaw,D. and Finch,J.T. (1993) A spacer protein in the *Saccharomyces cerevisiae* spindle pole body whose transcription is cell-cycle regulated. *J. Cell Biol.*, **123**, 1175–1184.

Knop,M. and Schiebel,E. (1997) Spc98p and Spc97p of the yeast γ-tubulin complex mediate binding to the spindle pole body via their interaction with Spc110p. *EMBO J.*, **16**, 6985–6995.

Knop,M. and Schiebel,E. (1998) Receptors determine the cellular localization of a γ-tubulin complex and thereby the site of microtubule formation. *EMBO J.*, **17**, 3952–3967.

Knop,M., Siegers,K., Pereira,G., Zachariae,W., Winsor,B., Nasmyth,K. and Schiebel,E. (1999) Epitope tagging of yeast genes using a PCR-based strategy: more tags and improved practical routines. *Yeast*, **15**, 963–972.

Lechner,J. (1994) A zinc-finger protein, essential for chromosome segregation, constitutes a putative DNA-binding subunit of the *Saccharomyces cerevisiae* kinetochore complex, CBF3. *EMBO J.*, **13**, 5203–5211.

Lechner,J. and Carbon,J. (1991) A 240kd multisubunit protein complex, CBF3, is a major component of the budding yeast centromere. *Cell*, **64**, 717–725.

Meluh,P.B. and Koshland,D. (1995) Evidence that the MIF2 gene of *Saccharomyces cerevisiae* encodes a centromere protein with homology to the mammalian centromere protein CENP-C. *Mol. Biol. Cell*, **6**, 793–807.

Meluh,P.B., Yang,P., Glowczewski,L., Koshland,D. and Smith,M.M. (1998) Cse4p is a component of the core centromere of *Saccharomyces cerevisiae*. *Cell*, **94**, 607–613.

Michaelis,C., Ciosk,R. and Nasmyth,K. (1997) Cohesins: chromosomal proteins that prevent premature separation of sister chromatids. *Cell*, **91**, 35–45.

Neff,N.F., Thomas,J.H., Grisafi,P. and Botstein,D. (1983) Isolation of the β-tubulin gene from yeast and demonstration of its essential function *in vivo*. *Cell*, **33**, 211–219.

Newman,J.R.S., Wolf,E. and Kim,P.S. (2000) A computationally directed screen identifying interacting coiled coils from *Saccharomyces cerevisiae*. *Proc. Natl Acad. Sci. USA*, **97**, 13203–12208.

Ortiz,J., Stemmann,O., Rank,S. and Lechner,J. (1999) A putative protein complex consisting of Ctf19, Mcm21, and Okp1 represents a missing link in the budding yeast kinetochore. *Genes Dev.*, **13**, 1140–1155.

Osborne,M.A., Schlenstedt,G., Jinks,T. and Silver,P.A. (1994) Nuf2, a spindle pole body-associated protein required for nuclear division in yeast. *J. Cell Biol.*, **125**, 853–866.

Pereira,G., Knop,M. and Schiebel,E. (1998) Spc98p directs the yeast

γ-tubulin complex into the nucleus and is subject to cell cycle-dependent phosphorylation on the nuclear side of the spindle pole body. *Mol. Biol. Cell*, **9**, 775–793.

Pereira,G., Grueneberg,U., Knop,M. and Schiebel,E. (1999) Interaction of the yeast γ-tubulin complex binding protein Spc72p with Kar1p is essential for microtubule function during karyogamy. *EMBO J.*, **18**, 4180–4196.

Pereira,G., Höfken,T., Grindlay,J., Manson,C. and Schiebel,E. (2000) The Bub2p spindle checkpoint links nuclear migration with mitotic exit. *Mol. Cell*, **6**, 1–10.

Pidoux,A.L. and Allshire,R.C. (2000) Centromeres: getting a grip of chromosomes. *Curr. Opin. Cell Biol.*, **12**, 308–319.

Rout,M.P. and Kilmartin,J.V. (1990) Components of the yeast spindle and spindle pole body. *J. Cell Biol.*, **111**, 1913–1927.

Sherman,F. (1991) Getting started with yeast. *Methods Enzymol.*, **194**, 3–21.

Shevchenko,A., Jensen,O.N., Podtelejnikov,A.V., Sagliocco,F., Wilm,M., Vorm,O., Mortensen,P., Boucherie,H. and Mann,M. (1996) Linking genome and proteome by mass spectrometry: large scale identification of yeast proteins from two dimensional gels. *Proc. Natl Acad. Sci. USA*, **93**, 14440–14445.

Sikorski,R.S. and Hieter,P. (1989) A system of shuttle vectors and yeast host strains designed for efficient manipulation of DNA in *Saccharomyces cerevisiae. Genetics*, **122**, 19–27.

Spang,A., Geissler,S., Grein,K. and Schiebel,E. (1996) γ-tubulin-like Tub4p of *Saccharomyces cerevisiae* is associated with the spindle pole body substructures that organize microtubules and is required for mitotic spindle formation. *J. Cell Biol.*, **134**, 429–441.

Spencer,F. and Hieter,P. (1992) Centromere DNA mutations induce a mitotic delay in *Saccharomyces cerevisiae*. *Proc. Natl Acad. Sci. USA*, **89**, 8908–8912.

Stemmann,O. and Lechner,J. (1996) The *Saccharomyces cerevisiae* kinetochore contains a cyclin–cdk complex homologue, as identified by *in-vitro* reconstitution. *EMBO J.*, **15**, 3611–3620.

Takahashi,K., Murakami,S., Chikashige,Y., Funabiki,H., Niwa,O. and Yanagida,M. (1992) A low copy number central sequence with strict symmetry and unusual chromatin structure in fission yeast centromere. *Mol. Biol. Cell*, **3**, 819–835.

Tanaka,T., Fuchs,J., Loidl,J. and Nasmyth,K. (2000) Cohesin ensures bipolar attachment of microtubules to sister centromeres and resists their precocious separation. *Nature Cell Biol.*, **2**, 492–499.

Taylor,S.S. and McKeon,F. (1997) Kinetochore localization of murine Bub1 is required for normal mitotic timing and checkpoint response to spindle damage. *Cell*, **89**, 727–735.

Taylor,S.S., Ha,E. and McKeon,F. (1998) The human homologue of Bub3 is required for kinetochore localization of Bub1 and a Mad3/Bub3-related protein kinase. *J. Cell Biol.*, **142**, 1–11.

Thompson,J.D., Gibson,T.J., Plewniak,F., Jeanmougin,F. and Higgins,D.G. (1997) The CLUSTAL_X windows interface: flexible strategies for multiple sequence alignment aided by quality analysis tools. *Nucleic Acids Res.*, **25**, 4876–4882.

Uhlmann,F., Wenic,D., Pouparet,M.-A., Koonin,E.V. and Nasmyth,K. (2000) Cleavage of cohesin by the CD clan protease separin triggers anaphase in yeast. *Cell*, **103**, 375–386.

Wang,Y.C. and Burke,D.J. (1995) Checkpoint genes required to delay cell division in response to nocodazole respond to impaired kinetochore function in the yeast *Saccharomyces cerevisiae*. *Mol. Cell. Biol.*, **15**, 6838–6844.

Westendorf,J.M., Rao,P.N. and Gerace,L. (1994) Cloning of cDNAs for M-phase phosphoproteins recognized by the MPM2 monoclonal antibody and determination of the phosphorylated epitope. *Proc. Natl Acad. Sci. USA*, **91**, 714–718.

Wigge,P.A., Jensen,O.N., Holmes,S., Souès,S., Mann,M. and Kilmartin,J.V. (1998) Analysis of the *Saccharomyces* spindle pole by matrix-assisted laser desorption/ionization (MALDI) mass spectrometry. *J. Cell Biol.*, **141**, 967–977.

Yamamoto,A., Guacci,V. and Koshland,D. (1996) Pds1p, an inhibitor of anaphase in budding yeast, plays a critical role in the APC and checkpoint pathway(s). *J. Cell Biol.*, **133**, 99–110.

Zheng,L., Chen,Y. and Lee,W.-H. (1999) Hec1p, an evolutionary conserved coiled-coil protein, modulates chromosome segregation through interaction with SMC proteins. *Mol. Cell. Biol.*, **19**, 5417–5428.

*Received November 2, 2000; revised November 28, 2000; accepted January 3, 2001*